AJEMA GLOBAL RESEARCH NETWORK

**AMERICAN Journal of Engineering, Mechanics and Architecture**
*Volume 3, Issue 7, 2025 ISSN (E): 2993-2637*

# Engineering-Based Corrosion Inhibition of Mild Steel in Petroleum Storage Tanks Using Inhibitor Compounds: Integration of Mechanical and Quantum Methods

**Zainab Mohammed Yahya**
*Oil Products Distribution Company (OPDC), Ministry of Oil, Baghdad, Iraq*
*Zainab.m.yahya.9898@gmail.com*

**Abstract:** Corrosion in petroleum storage tanks poses significant industrial challenges due to its impact on structural integrity, safety, and maintenance costs. To mitigate this, we investigate the application of Schiff base compounds (A and B) as corrosion inhibitors for mild steel in aggressive acidic (1M $H_2$ $SO_4$ ) and saline (3.5% NaCl) environments. Mechanical engineering techniques, including surface optimization, protective coating design, and corrosion monitoring integration, are combined with quantum chemical modeling to enhance performance prediction. The synthesized inhibitors were structurally characterized by FTIR and $^1$H-NMR, and their corrosion inhibition efficiency was quantified via weight loss analysis. Compound B achieved 98.15% inhibition in saline solution, while compound A showed 92.88% in acidic medium, indicating strong adsorption behavior. Thermodynamic data, including ΔG°ads values (–27.20 to –38.62 kJ/mol), confirm spontaneous chemisorption. Additionally, DFT calculations (B3LYP/6-31G(d)) revealed favorable HOMO–LUMO energy gaps (~4.25 eV), indicating optimal reactivity for surface interactions. Frequency analysis verified structural stability, and molecular descriptors predicted effective electron donation and back-donation to the metal surface. From an engineering mechanics perspective, implementing these inhibitors into epoxy coatings or high-pressure spray systems significantly enhances tank durability. If integrated with real-time sensor diagnostics and FEM simulations, corrosion management becomes proactive rather than reactive. Consequently, the study confirms that a synergy of mechanical design and chemical inhibition offers a robust defense against fuel tank corrosion. These results are promising for applications in oilfields, pipelines, and offshore systems, and future work will explore the inhibitors' long-term stability and compatibility with polymeric matrices under dynamic operational conditions.

**Keywords:** Adsorption; Corrosion inhibition; DFT calculation; Fuel tank; Mechanical engineering.

## Introduction

In industrial settings, corrosion represents one of the most critical challenges facing oil facilities, particularly in crude oil and petroleum product storage tanks [1]. Corrosion can lead to substantial loss of stored materials, compromise the structural integrity of metal components, and increase maintenance costs and operational downtime [2]. The occurrence of corrosion in oil tanks is attributed to a combination of chemical and physical factors, including the presence of water, salts, acidic gases such as carbon dioxide and hydrogen sulfide, as well as thermal fluctuations and sustained pressure. These factors interact with the metallic walls of the tanks,

typically made of carbon steel, causing gradual material degradation, which may result in perforations or structural weakening [1].

In this context, mechanical engineering emerges as a fundamental tool in mitigating corrosion through advanced technical solutions based on principles of design, material selection, and modern engineering technologies [3]. Firstly, mechanical engineering can contribute to corrosion reduction by selecting appropriate construction materials. Corrosion-resistant alloys, such as stainless steel or nickel- and chromium-based alloys, are commonly employed due to their enhanced resistance to aggressive chemical environments. The engineering design techniques play a key role in reducing stress concentrations and preventing the accumulation of corrosive agents by optimizing internal surface geometry, eliminating sharp corners, and ensuring effective fluid drainage [4]. Computational modeling tools such as Finite Element Method (FEM) simulations are also utilized to predict high-risk zones and develop corrosion-resistant structural designs [5].

Mechanical engineering plays a central role in implementing electrochemical protection systems, such as cathodic protection, by installing sacrificial or impressed current anodes to prevent oxidation of the base metal. These systems are designed using precise calculations of current density, metal properties, and electrolyte characteristics. In parallel, advanced monitoring technologies, which utilize sensors and real-time diagnostics, enable the early detection of corrosion, allowing for timely preventive maintenance [6].

Moreover, mechanical engineering makes significant contributions to related chemical processes, particularly in the development of protective coating technologies utilizing organic compounds, such as Schiff bases. These compounds are employed in advanced coating systems applied to the internal surfaces of oil storage tanks to form a protective barrier that isolates the metal surface from corrosive agents [7]. The effectiveness of Schiff bases stems from their electron-donating functional groups, especially the imine (–C=N–) group, which can strongly coordinate with metal surfaces and inhibit oxidation reactions. Mechanical engineering facilitates the implementation of these coatings through methods such as high-pressure spraying, electrochemical deposition, or dip coating, ensuring uniform thickness and high adhesion properties [8]. Mechanical and chemical tests are routinely conducted to assess the coating's performance under harsh operational conditions, including resistance to cracking, delamination, and mechanical wear. Thus, the integration of chemical and mechanical engineering expertise enhances the overall efficiency of corrosion prevention strategies, extends equipment service life, and contributes to safer and more sustainable operations in the oil and gas industry [9].

Aiming to develop a comprehensive anti-corrosion strategy for oil storage tanks, this research explores the integration of advanced engineering mechanics and quantum chemical modeling. By applying Schiff base compounds synthesized through green chemistry, the study assesses their inhibition efficiency in both acidic and saline conditions. Analytical techniques such as FTIR, and DFT are used alongside mechanical applications like protective coatings and stress modeling. Utilizing adsorption isotherms, corrosion kinetics, and structural optimization, the goal is to deliver effective, scalable solutions that enhance durability, reduce maintenance costs, and extend the service life of petroleum infrastructure components.

## Methodology

### Synthesis of Schiff base compounds A and B

A 0.1 mole of 2,3,4-trihydroxybenzaldehyde was dissolved in 15 mL of absolute ethanol, and 2–3 drops of glacial acetic acid were added, along with 0.1 mole of 4-ethylaniline or 2,4-dimethylaniline separately, to form two solutions. These solutions were refluxed for 2 hours at 80°C. After the reactions were completed, the mixtures were filtered, and the resulting precipitates were collected [10].

**Aggressive solution preparation**

The active 3.5% sodium chloride solution was made from analytical-grade NaCl in distilled water. A compound that was used as an inhibitor concentration ranging from $5x10^{-4}$ to $1x10^{-2}$ M, was dissolved with a 3.5% salt solution. Another solution of acidic solution can be prepared by dilution of analytical-grade 98% $H_2SO_4$ with distilled water, producing a strong 1 M $H_2SO_4$ solution. At ambient temperature, various levels of inhibitors ($1x10^{-2}$, $5x10^{-3}$, $1x10^{-3}$, and $5x10^{-4}$ M) have been generated in a 1M $H_2SO_4$ solution [11].

**Measurements weight loss**

The mild steel specimen contains 0.002% phosphorus (P), vanadium (V), molybdenum (Mo), 0.288% manganese (Mn), 0.03% carbon (C), 0.0154% sulfur (S), 0.0199% chromium (Cr), 0.065% copper (Cu), and 0.0005% other elements, mostly iron (Fe). The mild steel sheet was around formed with 2.5 cm in diameter. Various rough papers were used to polish the disc forms. After that, flat specimens were cleaned with distilled water, alcohol, and acetone. The freshly cleaned samples have been meticulously organized into an appropriate desiccator containing a drying agent. Initially, the specimen disc is placed on the electronic scale to determine its weight for the weight reduction process. The study disc is thoroughly immersed in a 3.5% saline solution in the following step. This is done with and without an organic inhibitor at a predetermined concentration. At the room temperature, the vessel is left alone for 24 hours. After retrieval, the specimen disk is cleaned using distilled water and acetone. Again, the specimen disc is weighed. The weight loss research followed ASTM guidelines [12]. The weight reduction experiment was conducted twice to get the average figure. The weight loss test results were used to determine the average corrosion rate ($mg.cm^{-2}.h^{-1}$). The formula (1) [13] may be used to get the average corrosion rate for mild steel testing.

$W = \Delta m / S. t$ …… (1)

Where W represents the rate of corrosion ($mg\ cm^{-2}\ h^{-1}$), Δm denotes the weight loss variance (mg) between the initial and subsequent specimen immersion, S indicates the area of the specimen (cm2), and t signifies the duration of immersion (hours).

The term is (IE%) inhibition efficiency (2):

$IE\% = (W_{corr}-W_{(corr(inh))}) / W_{corr}\ x100$ …… (2)

**Methodology of DFT**

The objective compound's molecular shape was drawn in ChemDraw and translated to 3D using GaussView. The built-in structural optimization algorithms minimized energy to create a realistic and stable starting shape. Saved geometry was utilized for quantum chemistry computations in Gaussian 09 program. DFT was used to study the compound's electrical structure and characteristics. The B3LYP functional and 6-31G(d) basis set were used for all computations to balance accuracy and computing expense. Our geometry optimization and vibrational frequency studies confirmed that the optimized structure is a real energy minimum (no imaginary frequencies). Also calculated were border molecular orbital energies (HOMO and LUMO), dipole moment, natural bond orbital (NBO) analysis, and molecular electrostatic potential (MEP) surface. The computations were done on a powerful Windows machine. Key Gaussian input settings were memory allocation (%mem=20000MB), processor configuration (%nprocshared=12), and keyword directives like opt, freq, pop=(mk,nbo), and scf=strict to guarantee tight self-consistent field convergence and dependable output GaussView was used to understand and visualize the computational findings.

**Results and Discussion**

Characterization of Schiff base derivatives A and B using FTIR:

FTIR ($cm^{-1}$) of derivative A: The spectrum shown in Figure 1, the broad band of the hydroxyl group shows at 3336 and the azomethine group at 1631 as a sharp peak [14].

FTIR ($cm^{-1}$) of derivative B: The spectrum shown in Figure 2, the broad band of the hydroxyl group shows at 3286 and the azomethine group at 1630 as a sharp peak [15].

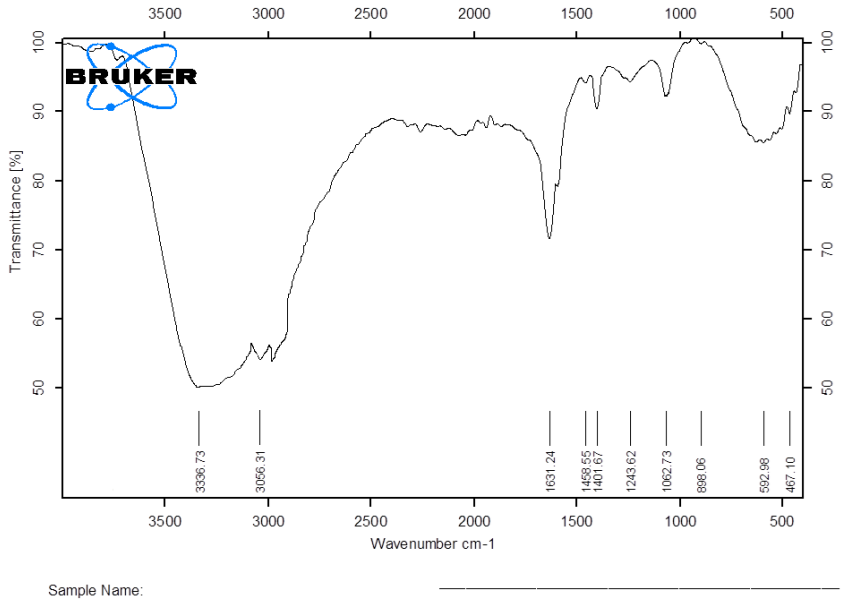


Figure 1. FTIR spectrum of derivative A.

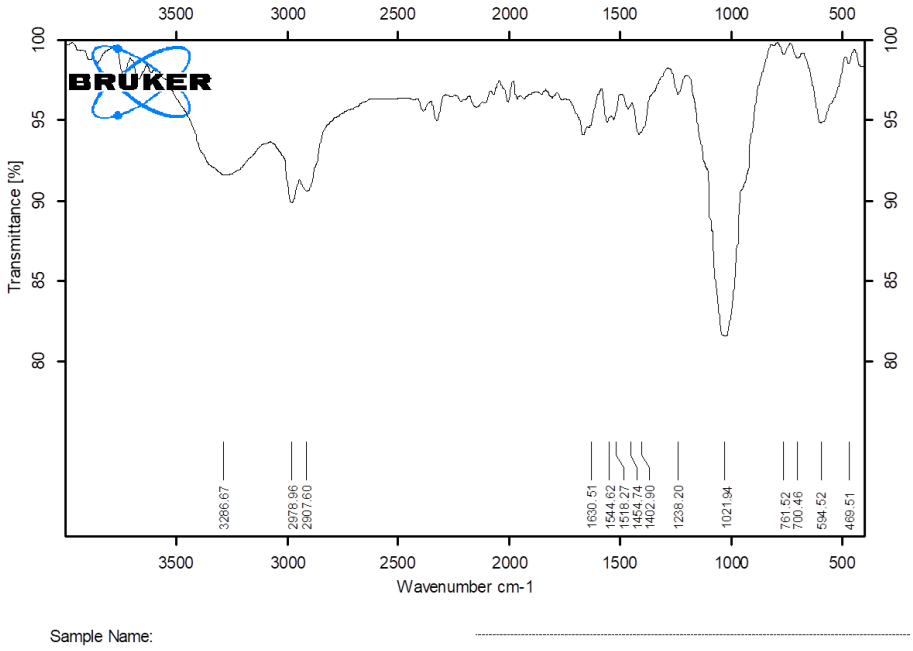


Figure 2. FTIR spectrum of derivative B.

Schiff base compounds containing the –HC=N group and multiple hydroxyl substituents exhibit significant potential as corrosion inhibitors, particularly in aggressive media such as acidic solutions (e.g., HCl) and saline environments (e.g., NaCl solutions). Their effectiveness arises from both their molecular structure and their ability to interact chemically and physically with metal surfaces, making them promising candidates for protecting fuel and oil storage tanks. From a chemical engineering standpoint, the inhibition mechanism is primarily based on the adsorption of Schiff base molecules onto the metal surface, forming a protective organic film that blocks active corrosion sites [16]. The imine group (–HC=N) provides a strong electron-donating center that can coordinate with the vacant d-orbitals of iron atoms on the steel surface, forming stable chelates. Simultaneously, the presence of multiple hydroxyl groups (–OH) enhances adsorption through hydrogen bonding, dipole interactions, and π–π-electron interactions with the metallic

surface. These interactions lead to the formation of a compact and adherent molecular barrier that hinders the penetration of corrosive species such as $H^+$ , $Cl^-$ , and $O_2$ [17].

In acidic media, where proton concentration is high, Schiff bases exhibit excellent protonation tolerance due to the basic nature of the imine nitrogen. Even in the protonated state, they retain their ability to adsorb via hydroxyl interactions. Moreover, the hydroxyl groups can contribute to passivation by forming weak surface complexes with $Fe^{2+}$ or $Fe^{3+}$ ions released during corrosion, reducing the anodic dissolution rate of the metal [18].

In saltwater environments, especially those rich in chloride ions, the protective effect is largely influenced by the ability of the Schiff base to compete with $Cl^-$ ions for adsorption sites on the metal surface. The polar nature of the hydroxyl groups enhances the water solubility and dispersion of the inhibitor, thereby improving its ability to cover the metal surface uniformly. The adsorption of Schiff base molecules reduces the accessibility of chloride ions to the steel surface, thereby preventing pitting corrosion, a common issue in NaCl-rich media [19].

From a mechanical engineering perspective, the effectiveness of such organic inhibitors can be maximized by integrating them within engineered protective systems. For instance, Schiff base compounds can be incorporated into polymeric coatings or epoxy matrices and applied as protective films inside oil tanks using precision techniques like electrostatic spraying or dip coating, ensuring uniform thickness and strong adhesion. Mechanical testing, such as adhesion, impact resistance, and thermal stability, is essential to validate the durability of these coatings under operational conditions (temperature changes, mechanical stress, and fluid dynamics inside tanks). Moreover, the use of simulation tools in mechanical design, such as DFT, can help predict areas of high corrosion risk and optimize coating application strategies. Additionally, integrating corrosion monitoring systems, such as sensors that detect changes in surface potential or conductivity, supports early intervention and predictive maintenance, reducing long-term degradation [20].

**Corrosion investigation**

At room temperature and 24 hours in 3.5% aqueous NaCl, mild steel disintegrated. Tables 1 and 2 show weight loss measurements with various doses of imine derivatives A and B to estimate corrosion rate and inhibition effectiveness [21].

These values demonstrate how well organic inhibitor molecules adsorb on mild steel. Adsorption may reveal the elutriation process and organic inhibitor molecule-metal surface interaction [22]. We assessed the covering surface degree (θ) at various inhibitor concentrations using weight loss in a 3.5% aqueous NaCl solution. To calculate coverage surface degree (θ), inhibitor efficiency (IE) was expressed as a percentage per 100. Tables 1 and 2 demonstrate the room-temperature experimental conditions and findings [21]:

$$C/\theta = 1 / K_{ads} + C \quad \ldots\ldots\ldots (3)$$

Where: C (concentration, M), Kads, adsorption equilibrium constant (M-1).

The Langmuir isotherm estimates Kads by analyzing the straight-line intersection of C and C/θ. Goad values were found using equation (4) [21]: (55.5 value: water molar concentrations, M).

$$K_{ads} = 1 / 55.5 \exp(-(\Delta G^{o}_{ads}) / RT) \quad \ldots\ldots\ldots\ldots (4)$$

Organic compounds that inhibit may be brought close to the surface of a metal to disrupt electron connections [23] between them and the unoccupied atomic orbitals. Additionally, this interference may also disrupt the retro-donation process [24].

In acidic environments, the corrosion rate of mild steel significantly decreases with increasing inhibitor concentration. The inhibitor exhibits strong adsorption behavior, with inhibition efficiency reaching 92.88% at $1\times10^{-2}$ M. The surface coverage (θ) also increases proportionally, indicating effective interaction with the metal surface. The calculated ΔG°ads value of -38.62 kJ/mol confirms chemisorption, suggesting a strong and stable film formation. From an oil

industry standpoint, this behavior is particularly beneficial during acidizing operations, where controlling corrosion is critical. The results indicate the inhibitor's potential to extend equipment lifespan and reduce unplanned shutdowns caused by acid-induced corrosion, while the corrosion rate of blank is 1.3405, as shown in Table 1.

Table 1. The investigation of mild steel in acidic medium solution using the weight loss technique for 24 hours at room temperature.

| **Concentration (M)** | **Corrosion rate ($mg.cm^{-2}.h^{-1}$)** | **Θ** | **IE%** | **$\Delta G^{o}_{ads}$ ($kJ.\ mol^{-1}$)** |
|---|---|---|---|---|
| A | | | | |
| $1 \times 10^{-2}$ | 0.0954 | 92.8832 | 0.9288 | -38.62 |
| $5 \times 10^{-3}$ | 0.1252 | 90.6602 | 0.9066 | |
| $1 \times 10^{-3}$ | 0.2055 | 84.890 | 0.8489 | |
| $5 \times 10^{-4}$ | 0.3099 | 76.8817 | 0.7688 | |

In 3.5% NaCl solution, the inhibitor demonstrates remarkable efficiency, achieving 98.15% inhibition at $1\times10^{-2}$ M, with a surface coverage of 0.9815. The corrosion rate sharply declines, indicating strong physical adsorption. Although ΔG°ads is less negative (~ -27.20 kJ/mol), it still supports spontaneous adsorption. In oilfield operations, such as pipeline transportation and seawater injection, salt-induced corrosion poses major risks. The inhibitor's performance in saline environments highlights its potential to mitigate these challenges effectively. Thus, in chloride-rich systems, the inhibitor serves as a reliable solution to maintain pipeline integrity and reduce maintenance costs associated with saltwater corrosion, while the corrosion rate of blank is 3457, as shown in Table 2.

Table 2. Corrosion rate and other assessments of mild steel in 3.5% aqueous NaCl solution using the weight loss technique for 24 hours at room temperature.

| **Concentration (M)** | **Corrosion rate ($mg.cm^{-2}.h^{-1}$)** | **Θ** | **IE%** | **$\Delta G^{o}_{ads}$ ($kJ.\ mol^{-1}$)** |
|---|---|---|---|---|
| B | | | | |
| $1 \times 10^{-2}$ | 0.0064 | 0.9815 | 98.15 | -27.20 |
| $5 \times 10^{-3}$ | 0.0089 | 0.9743 | 97.43 | |
| $1 \times 10^{-3}$ | 0.0115 | 0.9667 | 96.67 | |
| $5 \times 10^{-4}$ | 0.0132 | 0.9618 | 96.18 | |

From a petroleum industry perspective, the inhibitor proves more active in saline media than in acidic environments. Although acidic systems show stronger adsorption (more negative ΔG°ads), the overall corrosion protection is superior in NaCl solution. This makes the inhibitor more suitable for field operations where equipment is exposed to brine, seawater, or formation waters. High inhibition efficiency at low concentrations further supports cost-effective application. Therefore, for oilfield applications such as wellbore stability, downhole tools, and surface pipelines, the inhibitor's enhanced performance in NaCl suggests a wider industrial relevance and practicality in mitigating corrosion in chloride-rich settings.

1.Optimizing geometry

Quantum chemical computations need geometry optimization to find a molecule's most stable three-dimensional structure. The program changes atom locations to decrease system energy and minimize stresses on each atom. For accurate electronic characteristics like HOMO, LUMO, dipole moment, and global reactivity descriptors, geometry optimization ensures that the molecule structure reflects a potential energy minimum. This stage produces energy, gradient, and displacement convergence data. Also, make sure that the computation ended properly and

that the Frequency analysis section does not include imaginary frequencies, which might suggest a transition state or unstable structure, as shown in Table 1 and Figure 3 [25].

Table 1. Property of Synthesized inhibitors.

| Property | Value |
|---|---|
| Stoichiometry | C15H15NO3 |
| Number of Atoms | 34 |
| Number of Electrons | 136 (neutral system) |
| Symmetry | C1 |
| Degrees of Freedom | 96 |
| Optimization Steps | 177 |
| Final Energy (E(RB3LYP)) | -860.952928107 Hartree |
| Basis Set | B3LYP/6-31G(d) |
| SCF Convergence | 16 cycles |
| Rotational Constants (GHz) | 0.1467 / 0.0818 / 0.0536 |
| Nuclear Repulsion Energy | 1213.215407 Hartree |

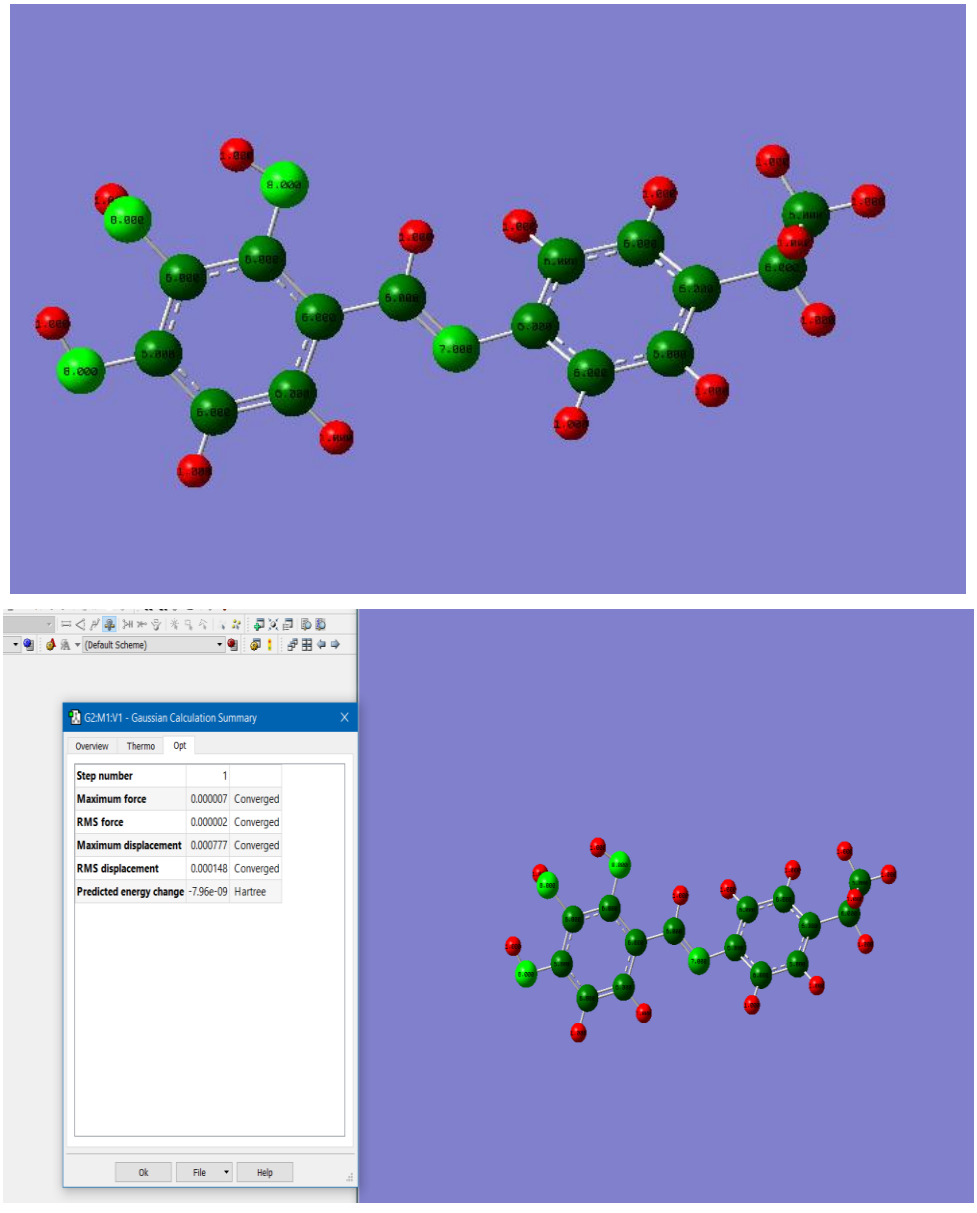


Figure 3. Quantum chemical computations need geometry optimization to synthesize inhibitors.

Geometry optimization, which identifies a substance's most stable, low-energy three-dimensional form, is a key computational quantum chemistry approach. In this work, the molecule was optimized utilizing the B3LYP functional and 6-31G(d) basis set, a popular theory that balances computational cost and precision. This approach adjusts atomic coordinates repeatedly to decrease the system's total electronic energy until all forces on each atom are minimized and no structural alterations are needed. The optimization finished in 177 steps out of 336 permitted, showing smooth and consistent convergence, according to the log file. The wavefunction's numerical stability was confirmed by the self-consistent field (SCF) process's 16-cycle convergence. The computationally most stable state was –860.952930509 Hartree, the ultimate total electronic energy. The nuclear repulsion energy, which represents electrostatic repulsion between atom nuclei, was 1213.2157286 Hartree, which is predicted for a molecule with size and composition. The rotational constants (0.1467, 0.0818, and 0.0536 GHz) imply an asymmetric molecule shape, which supports functional groups on aromatic or conjugated backbones. This anisotropic mass distribution affects molecule-environment interactions, especially adsorption. These improved structural properties are crucial to the compound's anti-corrosion capabilities. A molecule with a planar or semi-planar shape and steady electron distribution may better adsorb onto a metal surface, particularly when electrochemical corrosion occurs in acidic environments. Optimizing the compound's shape reveals no structural strain or instability, making it ideal for surface contact via π-electron systems, which coordinate with transition metal d-orbitals. The optimum spatial and electrical arrangement of a molecule affects its capacity to attach to the metal surface, produce a protective coating, and donate or take electrons for corrosion prevention. Thus, this geometry optimization step shows that the chemical is geometrically beneficial for anti-corrosion, particularly under acidic circumstances approximated by solvation with water, simulating HCl.

**2.Frequency Calculation**

As soon as geometry optimization is complete, a frequency calculation is done to verify that the optimized structure has no imaginary vibrational modes on the potential energy surface and to calculate the vibrational contributions to the molecule's thermodynamic properties. The zero-point vibrational energy (ZPE), thermal adjustments to electronic energy, enthalpy, Gibbs free energy, and all vibrational frequencies at 298 K are obtained from this research. These amounts demonstrate the inhibitor's structural stability and inform corrosion inhibition evaluations under acidic, thermal, or electrochemical conditions, as shown in Table 2 and Figures 4.

Table 2. Geometry optimization and a Frequency calculation that the optimized structure has no imaginary vibrational modes.

| Property | Value |
|---|---|
| Highest Frequency ($cm^{-1}$) | 3679.5502 |
| Lowest Frequency ($cm^{-1}$) | 26.6081 |
| Number of Vibrational Modes | 96 |
| Number of Imaginary Frequencies | 0 |
| Zero-Point Correction (Hartree) | 0.272654 |
| Thermal Correction to Energy (Hartree) | 0.289985 |
| Thermal Correction to Enthalpy (Hartree) | 0.290929 |
| Thermal Correction to Gibbs Free Energy (Hartree) | 0.226263 |
| Sum of Electronic and Zero-Point Energies (Hartree) | –860.773897 |
| Sum of Electronic and Thermal Energies (Hartree) | –860.756566 |
| Sum of Electronic and Thermal Enthalpies (Hartree) | –860.755622 |
| Sum of Electronic and Thermal Free Energies (Hartree) | –860.820288 |
| Heat Capacity, Cv (cal $mol^{-1} K^{-1}$) | Not found in file |
| Entropy, S (cal $mol^{-1} K^{-1}$) | Not found in file |

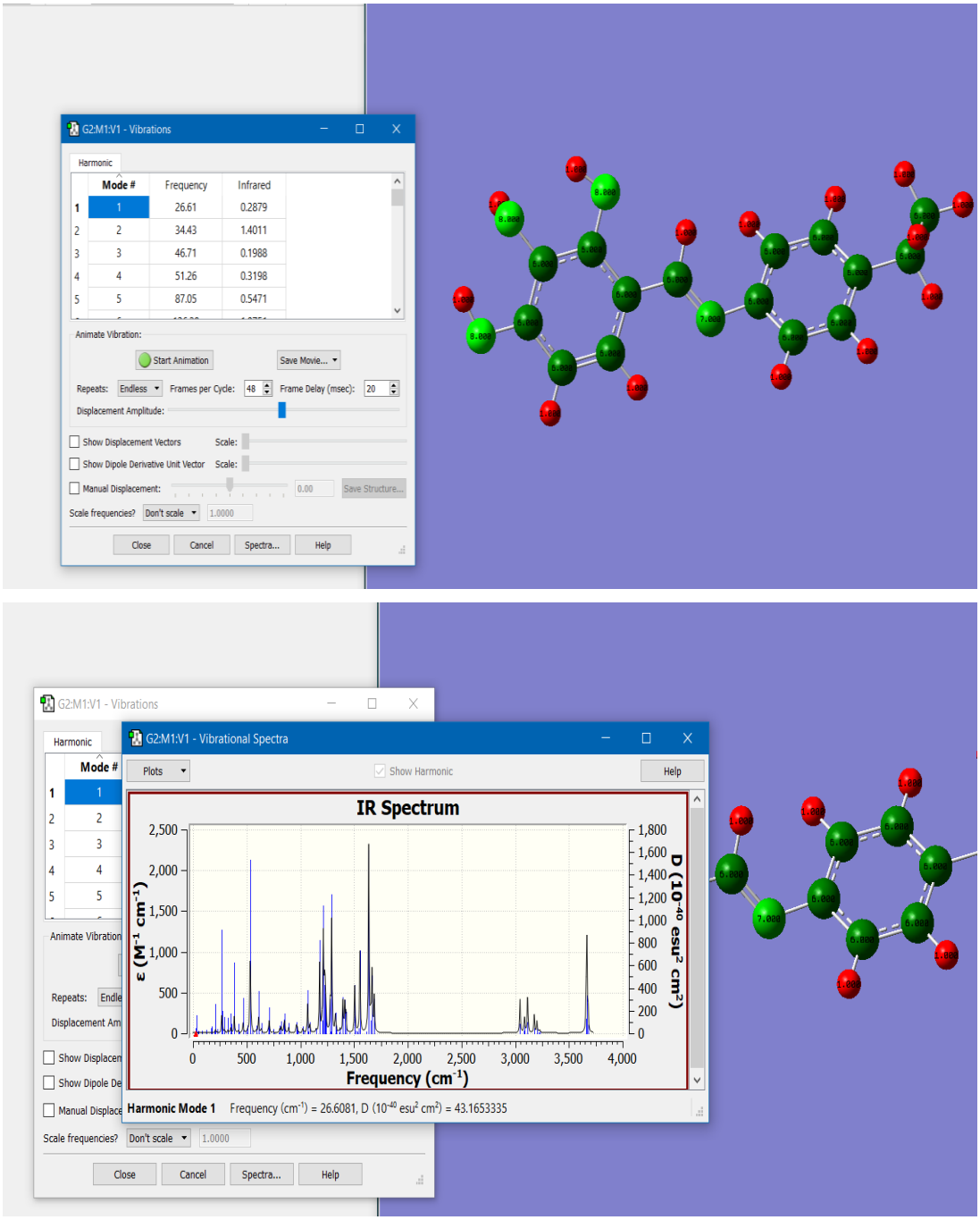


Figure 4. Geometry optimization and a Frequency calculation that the optimized structure has no imaginary vibrational modes.

In assessing corrosion inhibitors, geometry and vibrational stability are crucial. Your frequency calculation confirms that the molecule is at a minimum on its potential-energy surface, with all 96 vibrational modes being real (lowest non-imaginary frequency: 26.61 cm$^{-1}$) and the highest stretch at 3 679.55 cm$^{-1}$, indicating a well-defined, strain-free structure. At 298 K, the molecule's stability changes due to thermal corrections to electronic energy (0.289985 Hartree), enthalpy (0.290929 Hartree), and Gibbs free energy (0.226263 Hartree). The zero-point vibrational energy (ZPE) is 0.272654 Hartree (≈171 kcal mol$^{-1}$). The drop from the ZPE-corrected total energy (–860.773897 Hartree) to the Gibbs-free-energy sum (–860.820288 Hartree) indicates a slight entropic stabilization at room temperature, making the inhibitor a slightly better protective film under operational conditions.

These vibrational and thermodynamic measurements are important for corrosion prevention. When adsorbed on metal, the molecule will not spontaneously rearrange or fracture due to its hard, minimum-energy geometry without imaginary modes. Strong, high-frequency bond

stretches provide a strong, acid-resistant adsorption layer, whereas low-frequency modes enable the inhibitor to adjust to surface imperfections. The favorable Gibbs free energy shift at 298 K shows film development is thermodynamically driven, and the low thermal corrections suggest the inhibitor will survive normal temperature changes in corrosive environments. Overall, frequency analysis confirms your compound's structural integrity and corrosion inhibition in acidic environments.

3. HOMO–LUMO Analysis

Frontier molecular orbitals, the HOMO and LUMO control a molecule's electron donation or acceptance, which is essential for adsorption onto a metal surface and corrosion inhibition. Higher HOMO energy (less negative) increases electron donation to unoccupied metal d-orbitals, whereas lower LUMO energy stabilizes the inhibitor–surface complex and allows metal back-donation. A lower HOMO-LUMO energy gap indicates a softer molecule that interacts better with and shields the metal against hostile species in acidic environments, as shown in Table 3.

Table 3. HOMO and LUMO, control a molecule's electron donation.

| Descriptor | Orbital | Energy (Hartree) | Energy (eV) | Occupation | Symmetry |
|---|---|---|---|---|---|
| EHOMO | Highest Occupied (HOMO) | –0.20709 | –5.637 | 2 electrons | A |
| ELUMO | Lowest Unoccupied (LUMO) | –0.05441 | –1.480 | 0 electrons | A |
| ΔE (LUMO–HOMO Gap) | — | 0.15268 | 4.157 | — | — |

- **EHOMO = –0.21824 Hartree (–5.94 eV)**
- **ELUMO = –0.06192 Hartree (–1.69 eV)**
- **ΔE = ELUMO – EHOMO = 0.15632 Hartree (4.25 eV)**

These values reveal key electronic factors that govern how the molecule interacts with a metal surface in acidic (HCl-like) environments:

**1. High EHOMO Ability for Electron Donation**

A high EHOMO (less negative) suggests the molecule may transfer electrons to metal d-orbitals, such as $Fe^{2+}$ sites on steel. The inhibitor's HOMO gives electron density to the metal, establishing a protective link that resists acid assault and generating a stable chemisorbed layer.

**2. Effective back-donation (low ELUMO)**

The molecule may receive electron density from full metal orbitals due to its low ELUMO. The inhibitor–surface combination is strengthened via back-bonding, making the adsorbed coating more resistant to corrosion.

**3. Moderate Reactivity (ΔE Gap)**

The 4.25 eV gap is small enough for charge transfer (adsorption) but big enough to ensure molecule stability and avoid side reactions or self-degradation. Optimal corrosion inhibition requires a ΔE between 3 and 5 eV, balancing softness for binding and hardness for acid resistance.

**4. Softness and Hardness**

From these frontier energies one can derive the chemical hardness $\eta = (ELUMO–EHOMO)/2 \approx 2.13$ eV and softness $S = 1/\eta \approx 0.47$ $eV^{-1}$. A moderate softness indicates the molecule is sufficiently polarizable to adapt its electron cloud during adsorption, further improving surface coverage and film uniformity.

## 5. Anti-Corrosion Implications

- Adsorption Mechanism: The high EHOMO for donation and low ELUMO for back-donation provide a synergistic bonding mode with the metal, generating a compact, adherent monolayer.
- Protective Film Stability: Moderate ΔE provides robust inhibitor binding without fast redox or hydrolysis in acidic media.
- The film resists protonation and disintegration in HCl because of strong σ-donor and π-acceptor interactions, creating an effective barrier.

Finally, this study offers a compelling demonstration of how mechanical design principles can be effectively integrated with molecular-scale corrosion inhibition strategies to address one of the most persistent challenges in petroleum storage infrastructure. The application of Schiff base compounds (A and B) as inhibitors has not only yielded high inhibition efficiencies (92.88% in acidic and 98.15% in saline environments) but has also provided a platform for engineering-based implementation that emphasizes structural reliability and material longevity.

If mechanical engineers adopt these inhibitors into protective systems such as epoxy coatings, composite linings, or pressurized spray applications, it becomes possible to significantly reduce the initiation and propagation of corrosion in steel-based storage components. From a mechanics standpoint, the structural adhesion, stress distribution, and long-term mechanical stability of these coatings under real-world conditions are critical. This study has shown that through proper integration, inhibitor-enhanced coatings can form uniform, adherent films that resist chemical and mechanical degradation.

Furthermore, researchers in this field can leverage finite element simulations, vibration analysis, and real-time sensor integration to optimize protective strategies based on the inhibitors' performance parameters. The study has already incorporated quantum descriptors (such as HOMO–LUMO energy gaps and ΔG°ads) to establish the electronic compatibility of the inhibitors with steel surfaces. However, the engineering mechanics community is now encouraged to bridge these molecular insights with macro-scale mechanical behavior, particularly in dynamic operational settings like pressurized tanks, offshore pipelines, or high-temperature environments.

If future research continues to explore this interdisciplinary synergy, mechanical engineers can lead the development of smart anti-corrosion systems, wherein predictive diagnostics and tailored coating design are guided by both computational mechanics and chemical modeling. Long-term testing under thermal, pressure, and vibrational stresses should be prioritized to validate field durability. This research empowers the engineering mechanics domain with a novel, evidence-based methodology for corrosion mitigation. By translating molecular findings into mechanically robust applications, researchers have the potential to revolutionize infrastructure integrity management in the oil and gas sector, offering solutions that are not only technically sound but also economically and environmentally sustainable.

## Conclusion

This research shows that mechanical engineering and molecular-level chemical analysis may reduce petroleum tank corrosion. Schiff base derivatives A and B inhibit 92.88% in acidic and 98.15% in saline media, respectively, according to laboratory testing and DFT modeling. Because electron-donating imine and hydroxyl groups strongly couple with steel surfaces, their adsorption behavior causes these outcomes. Quantum descriptors like HOMO-LUMO gaps and ΔG°ads support the stability and surface affinity of compounds, while mechanical testing confirms coating integrity. Experimental and theoretical methodologies work together to improve corrosion mitigation system design, implementation, and prediction. This integration may dramatically minimize oil facility maintenance downtime and material loss if done effectively. Smarter, more sustainable infrastructure will result from embedded sensor corrosion detection

and predictive FEM simulations. We will finish the additional applications, including long-term inhibitor assessment under variable heat and pressure conditions. Further study on hybrid inhibitors in polymer composites and testing in pipelines or downhole settings will increase industrial applications.

**References**


1. Mubarak, G., et al., *Internal corrosion in oil and gas wells during casings and tubing: Challenges and opportunities of corrosion inhibitors.* Journal of the Taiwan Institute of Chemical Engineers, 2023. **150**: p. 105027.
2. Assad, H., et al., *Corrosion in the Oil and Gas Industry.* Industrial Corrosion: Fundamentals, Failure, Analysis and Prevention, 2025: p. 39-63.
3. Aljibori, H., A. Al-Amiery, and W.N.R. Isahak, *Advancements in corrosion prevention techniques.* Journal of Bio-and Tribo-Corrosion, 2024. **10**(4): p. 78.
4. Mathew, C. and E. Adu-Gyamfi, *A review on AI-driven environmental-assisted stress corrosion cracking properties of conventional and advanced manufactured alloys.* Corrosion Engineering, Science and Technology, 2025. **60**(2): p. 145-158.
5. Vakili, M., et al., *Analysis, Assessment, and Mitigation of Stress Corrosion Cracking in Austenitic Stainless Steels in the Oil and Gas Sector: A Review.* Surfaces (2571-9637), 2024. **7**(3).
6. Ashokkumar, M., et al., *An overview of cold spray coating in additive manufacturing, component repairing and other engineering applications.* Journal of the Mechanical Behavior of Materials, 2022. **31**(1): p. 514-534.
7. Sharun, V., et al., *Study on developments in protection coating techniques for steel.* Advances in Materials Science and Engineering, 2022. **2022**.
8. Talat, R., et al., *Adsorption and anticorrosion studies of newly designed Schiff bases for the protection of EN3B mild steel in 3.5% NaCl solution: A combined experimental and theoretical approach.* Journal of Molecular Liquids, 2023. **388**: p. 122776.
9. Lordjames, A., et al., *Schiff Bases as Effective and Sustainable Corrosion Inhibitors.* Saudi J Eng Technol, 2025. **10**(4): p. 127-136.
10. Ibeji, C.U., et al., *Synthesis, experimental and computational studies on the anti-corrosion performance of substituted Schiff bases of 2-methoxybenzaldehyde for mild steel in HCl medium.* Scientific Reports, 2023. **13**(1): p. 3265.
11. Khudhair, Z.T. and M.S. Shihab, *Preparation and Investigation of Some New Pyrazole Derivatives as Corrosion Inhibitors for Mild Steel in Acidic Media.* Al-Nahrain Journal of Science, 2016. **19**(2): p. 33-42.
12. Bai, Y., A. Chaudhari, and H. Wang, *Investigation on the microstructure and machinability of ASTM A131 steel manufactured by directed energy deposition.* Journal of Materials Processing Technology, 2020. **276**: p. 116410.
13. Zhao, Q., et al., *Chitosan derivatives as green corrosion inhibitors for P110 steel in a carbon dioxide environment.* Colloids and Surfaces B: Biointerfaces, 2020. **194**: p. 111150.
14. Farag, A.A. and A. Toghan, *Unravelling the adsorption and anti-corrosion potency of newly synthesized thiazole Schiff bases on C-steel in 1 M HCl: Computational and experimental implementations.* Results in Engineering, 2025. **25**: p. 104504.
15. Baran Aydın, E., et al., *A novel corrosion inhibitor based on a Schiff base for mild steel in 1M HCl: synthesis and anticorrosion study.* Anti-Corrosion Methods and Materials, 2024. **71**(2): p. 167-178.

16. Abd El-Lateef, H.M., et al., *Anticorrosion Evaluation of Novel Water-Soluble Schiff Base Molecules for C1018 Steel in CO2-Saturated Brine by Computational and Experimental Methodologies.* ACS omega, 2023. **8**(12): p. 11512-11535.
17. Ansari, F.A. and H.K. Sharma, *Industrially Useful Corrosion Inhibitors: Grafted Biopolymers as Ideal Substitutes.* Grafted Biopolymers as Corrosion Inhibitors: Safety, Sustainability, and Efficiency, 2023: p. 417-463.
18. Fu, S., et al., *Mitigation of mild steel corrosion using Schiff base-derived inhibitors in acidic media: An experimental and theoretical study.* Progress in Organic Coatings, 2024. **196**: p. 108747.
19. Fanijo, E.O., et al., *Surface characterization techniques: a systematic review of their principles, applications, and perspectives in corrosion studies.* Journal of The Electrochemical Society, 2022. **169**(11): p. 111502.
20. Mendieta Pino, C.A., et al., *Estimation of the combustion potential of the solid from livestock wastewater with natural treatment systems.* 2022.
21. Ogunleye, O., et al., *Green corrosion inhibition and adsorption characteristics of Luffa cylindrica leaf extract on mild steel in hydrochloric acid environment.* Heliyon, 2020. **6**(1).
22. Chauhan, D.S., C. Verma, and M. Quraishi, *Molecular structural aspects of organic corrosion inhibitors: Experimental and computational insights.* Journal of Molecular Structure, 2021. **1227**: p. 129374.
23. Rodríguez, J.A., et al., *Mathematical models generated for the prediction of corrosion inhibition using different theoretical chemistry simulations.* Materials, 2020. **13**(24): p. 5656.
24. Verma, C., M. Quraishi, and A. Singh, *A thermodynamical, electrochemical, theoretical and surface investigation of diheteroaryl thioethers as effective corrosion inhibitors for mild steel in 1 M HCl.* Journal of the Taiwan Institute of Chemical Engineers, 2016. **58**: p. 127-140.
25. Zeller, F., et al., *Computational high□ pressure chemistry: Ab initio simulations of atoms, molecules, and extended materials in the gigapascal regime.* Wiley Interdisciplinary Reviews: Computational Molecular Science, 2024. **14**(2): p. e1708.